Different approaches to synthesise cerium oxide nanoparticles and their corresponding physical characteristics, ROS scavenging and anti-inflammatory capabilities

Journal of
Materials Chemistry B

Materials for biology and medicine

Accepted Manuscript

This article can be cited before page numbers have been issued, to do this please use: Y. Wu and H. T. Ta, *J. Mater. Chem. B*, 2021, DOI: 10.1039/D1TB01091C.

ROYAL SOCIETY OF CHEMISTRY

rsc.li/materials-b

Different approaches to synthesise cerium oxide nanoparticles and their corresponding physical characteristics, ROS scavenging and anti-inflammatory capabilities

Yuao Wu[1], Hang T. Ta[1,2,3*]

[1]Queensland Micro- and Nanotechnology, Griffith University, Nathan, Queensland 4111, Australia

[2]School of Environment and Science, Griffith University, Nathan, Queensland 4111, Australia

[3]Australian Institute for Bioengineering and Nanotechnology, the University of Queensland, St Lucia, Queensland 4072, Australia

Abstract

The biological applications of cerium oxide nanoparticles (nanoceria) have received extensive attention in recent decades. The coexistence of trivalent cerium and tetravalent cerium on the surface of nanoceria allows the scavenging of reactive oxygen species (ROS). The regeneratable changes between the Ce^{3+} and Ce^{4+} make nanoceria a suitable treatment for ROS-related diseases and inflammatory diseases. The size, morphology and Ce^{3+}/Ce^{4+} state of the cerium oxide nanoparticles are affected by the synthesis method. This review focuses on various synthesis methods of cerium oxide nanoparticles and discusses their corresponding physical characteristics, anti-ROS and anti-inflammatory properties.

Keywords: cerium oxide nanoparticles, synthesis methods, physical characteristics, reactive oxygen species, anti-inflammation

1 Introduction

View Article Online
DOI: 10.1039/D1TB01091C

Cerium is a lanthanide element and a rare earth metal. Its oxides can be CeO_2 and Ce_2O_3 as cerium can be either trivalent (Ce^{3+}) or tetravalent (Ce^{4+})[1]. Cerium oxide is widely used as a polishing agent[2], catalyst[3], preservative[4], and sensor[5] in industry. With the development of the nanotechnology[6, 7], the biomedical applications of cerium oxide nanoparticles have been increasingly reported.[8, 9] Studies showed that nanoceria could be used as superoxide dismutase (SOD) mimetics[10], catalase (CAT) mimetics[11], scavenger of nitric oxide radicals[12] and hydroxyl radicals[13].

Since the concept of reactive oxygen species (ROS) was proposed in 1947, researches on active oxidants and antioxidants have not been interrupted in these decades.[14] Excess ROS has emerged as a critical factor in many chronic diseases, such as atherosclerosis[15], rheumatoid arthritis[16], hepatitis[17] and other inflammatory diseases[18]. Recently, the anti-ROS and anti-inflammatory properties of cerium oxide nanoparticles have been investigated and confirmed by several studies.[19-21] A number of novel synthesis methods of cerium oxide nanomaterials have also been reported.[22] The characteristics and functions of cerium oxide nanomaterials were shown related to their synthesis methods.

Cerium oxide nanoparticles are unique due to its convertible surface. Both trivalent cerium atoms (Ce^{3+}) and tetravalent cerium atoms (Ce^{4+}) are on the surface of cerium oxide.[23] Ce^{3+} on the surface works as an analogue of superoxide dismutase. It can transform superoxide radicals into oxygen and hydrogen peroxide ($Ce^{3+} + O_2^{-\bullet} + 2H^+ \rightarrow Ce^{4+} + H_2O_2$). It was also reported that Ce^{3+} could reduce H_2O_2 to H_2O. ($2Ce^{3+} + H_2O_2 + 2H^+ \rightarrow 2Ce^{4+} + 2H_2O$). Ce^{4+} produced by above reactions can also scavenge hydrogen peroxide and generate oxygen and water, eventually eliminating ROS. Due to the absorption of hydrogen electrons, the Ce^{4+} is then converted into the original Ce^{3+} ($2Ce^{4+} + H_2O_2 + 2OH^- \rightarrow 2Ce^{3+} + O_2 + 2H_2O$)[10] (Fig 1A). Hence, this irreplaceable anti-ROS property allows cerium oxide to be utilised as a potential regenerative ROS scavenger.[24-29]

There are few reviews discussing synthesis[30, 31] and biomedical applications[32, 33] of cerium oxide nanoparticles. However, as research interest in anti-ROS and anti-inflammation properties of nanoceria increases, a review with a detailed discussion between its synthesis, surface valence, anti-ROS and anti-inflammation is urgently needed. Our review fills this gap. In this review, typical synthesis methods and also novel green synthesis methods of cerium oxide nanoparticles are comprehensively discussed (Figure 1B). The size, morphology and Ce

View Article Online
DOI: 10.1039/D1TB01091C

$^{3+}$/Ce $^{4+}$ state of cerium oxide nanoparticles are compared between different synthesis methods. Then the anti-ROS and anti-inflammatory ability of cerium oxides nanoparticles are reviewed. Lastly, the future expectation of cerium oxide nanoparticles are discussed.

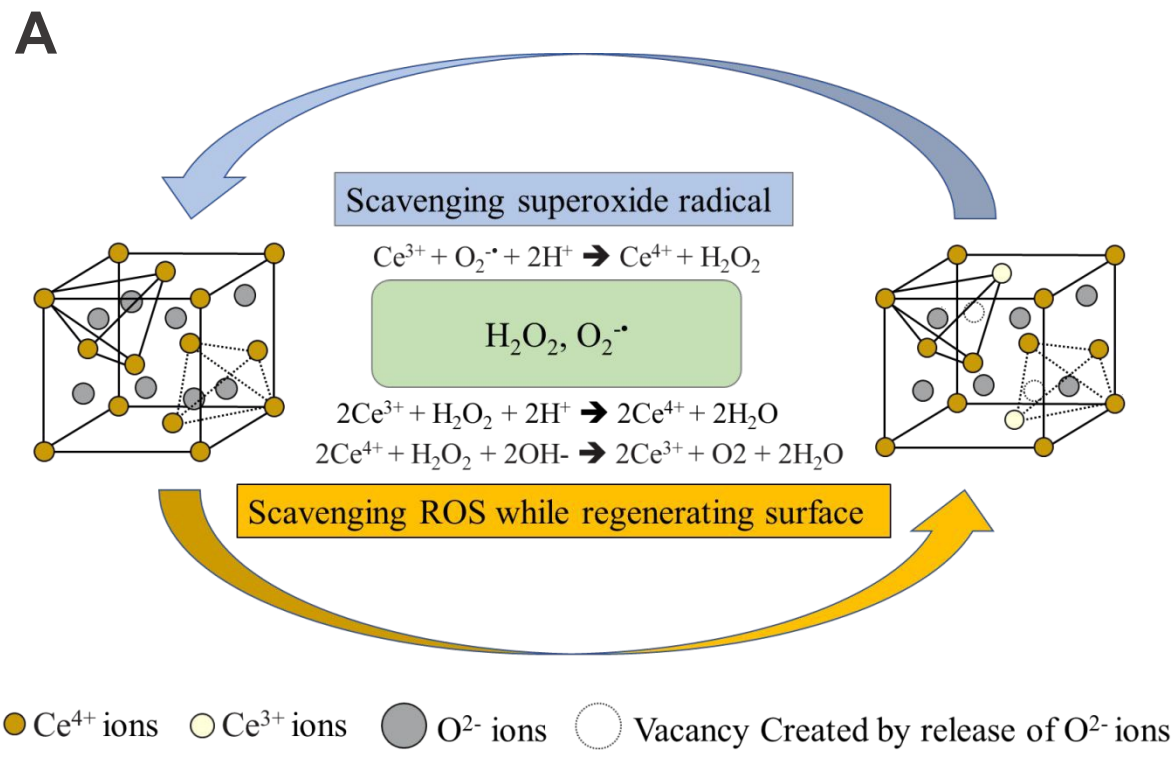

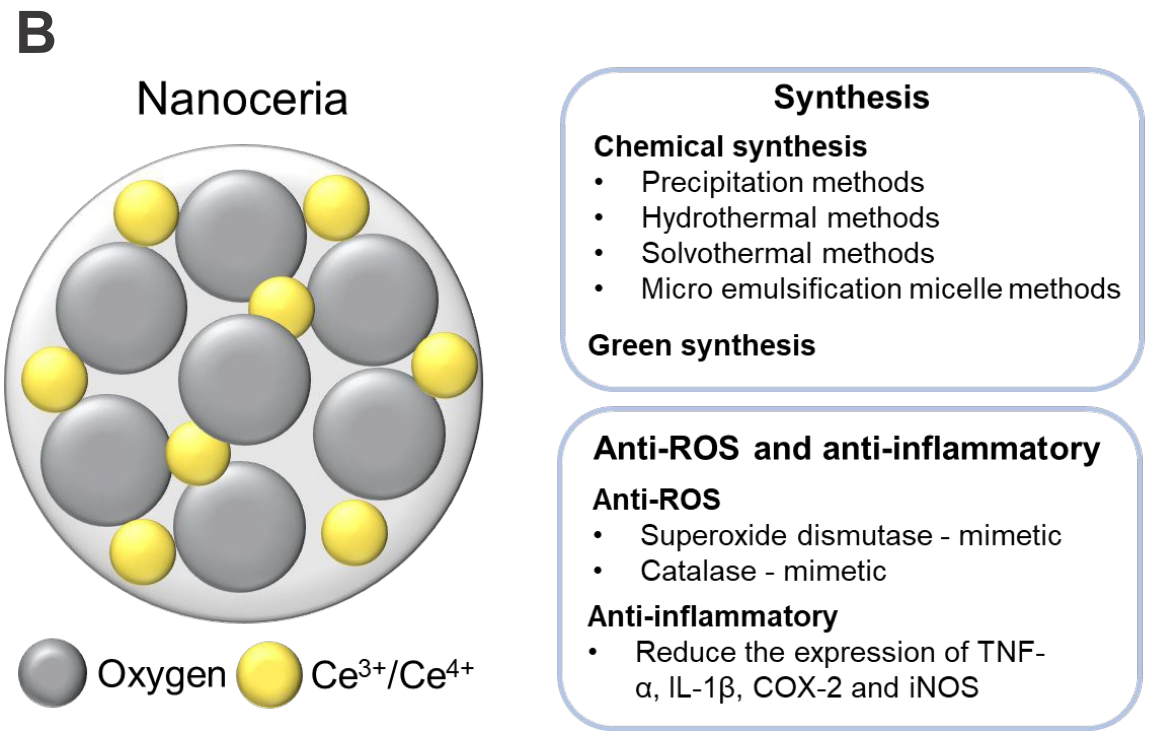

Fig 1. Overview of cerium oxide nanoparticles. (A) Regenerative antioxidant property of cerium oxide nanoparticles. **(B)** Synthesis and anti-ROS, anti-inflammatory properties of cerium oxide nanoparticles.

2 Synthesis of cerium oxide nanoparticles

Various methods of synthesising cerium oxide nanoparticles have been reported in the last decades. Studies indicated that different synthesis methods could affect the size, morphology and surface valence of the cerium oxide nanoparticles. Conventional chemical synthesis is the major approach of synthesising nanoceria. Recently, novel bio-directed synthesis methods (green synthesis) have also been reported.

2.1 Conventional chemical synthesis

Numerous of chemical synthesis methods of cerium oxide nanoparticles were described, including precipitation[34-36], hydrothermal[37-39], solvothermal[40], sol-gel[41] and micro emulsification micelle methods[42].

2.1.1 Precipitation methods

Table 1 summarises precipitation methods used for synthesis of cerium oxide nanoparticles. In the precipitation reaction, nanoceria is obtained by adding reactant ligands (such as sodium hydroxide or ammonium hydroxide) to the metal ion solution (precursors). Cerium (III) nitrate hexahydrate is one of the most used precursors. In a study by Lin et al.[43], the effect of reactant ligand was reported. Sodium hydroxide or ammonium hydroxide was reacted with cerium (III) nitrate hexahydrate separately. Results suggested that the nanoceria synthesised by ammonium hydroxide had smaller size compared to the ones synthesised by sodium hydroxide. Ammonium-involved nanoceria also had better stability and regular spherical shape. Large agglomeration of particles was observed in sodium hydroxide-derived nanoceria. In another study where precipitation method was applied, Yurova et al.[44] sought to investigate the effect of precursors and acidic modifications on cerium oxide nanoparticles. In the reaction, ammonium cerium (IV) nitrate and cerium (III) nitrate hexahydrate was used as two different sources of nanoceria. Transmission electron microscopy (TEM) images showed cerium (III)-derived nanoceria has the bigger size (6-12nm) than cerium (IV)-derived nanoceria (2-3nm). The morphology of nanoparticles could be changed from hexagons to spherical or ellipsoidal when particles were treated with sulphate acid and phosphate acid. In addition, poly(acrylic

View Article Online
DOI: 10.1039/D1TB01091C

acid) has been reported to be the common coating of the cerium oxide nanoparticles. The resulting nanoparticles were synthesised by ammonium cerium (IV) nitrate and ammonium hydroxide and had hydrodynamic diameter of 6 nm and have both Ce^{3+} and Ce^{4+} on the surface.[45]

Table 1. Synthesis of cerium oxide nanoparticles using precipitation methods.

Precursors		**Reactant**		**Size (nm)**	**Surfactant/ coating**	**Morphology**	**Valence states**	**Ref.**
Cerium(III) nitrate hexahydrate (mol/L)	0.4	Ammonium hydroxide (mol/L)	0.4	13-33	Citrate acid/EDTA	Nanosphere	Ce3+ & Ce4+	43
Cerium(III) nitrate hexahydrate (mol/L)	0.2	Ammonium hydroxide (mol/L)	2.3	12	N/A	Nanohexagon	Ce3+ & Ce4+	44
	0.2		2.3	6	Monosodium phosphate	Nanosphere		
	0.2		2.3	7	Sodium bisulfate	Nanosphere		
Ammonium cerium(IV) nitrate	0.2		2.3	2.6	N/A	Nanohexagon		
	0.2		2.3	2.7	Monosodium phosphate	Nanosphere		
	0.2		2.3	2.6	Sodium bisulfate	Nanosphere		
Ammonium cerium(IV) nitrate	0.11	Ammonium hydroxide (mol/L)	9.8	6	Poly(acrylic acid)	Nanosphere	Ce3+: Ce4+ 1.28:1	45

View Article Online
DOI: 10.1039/D1TB01091C

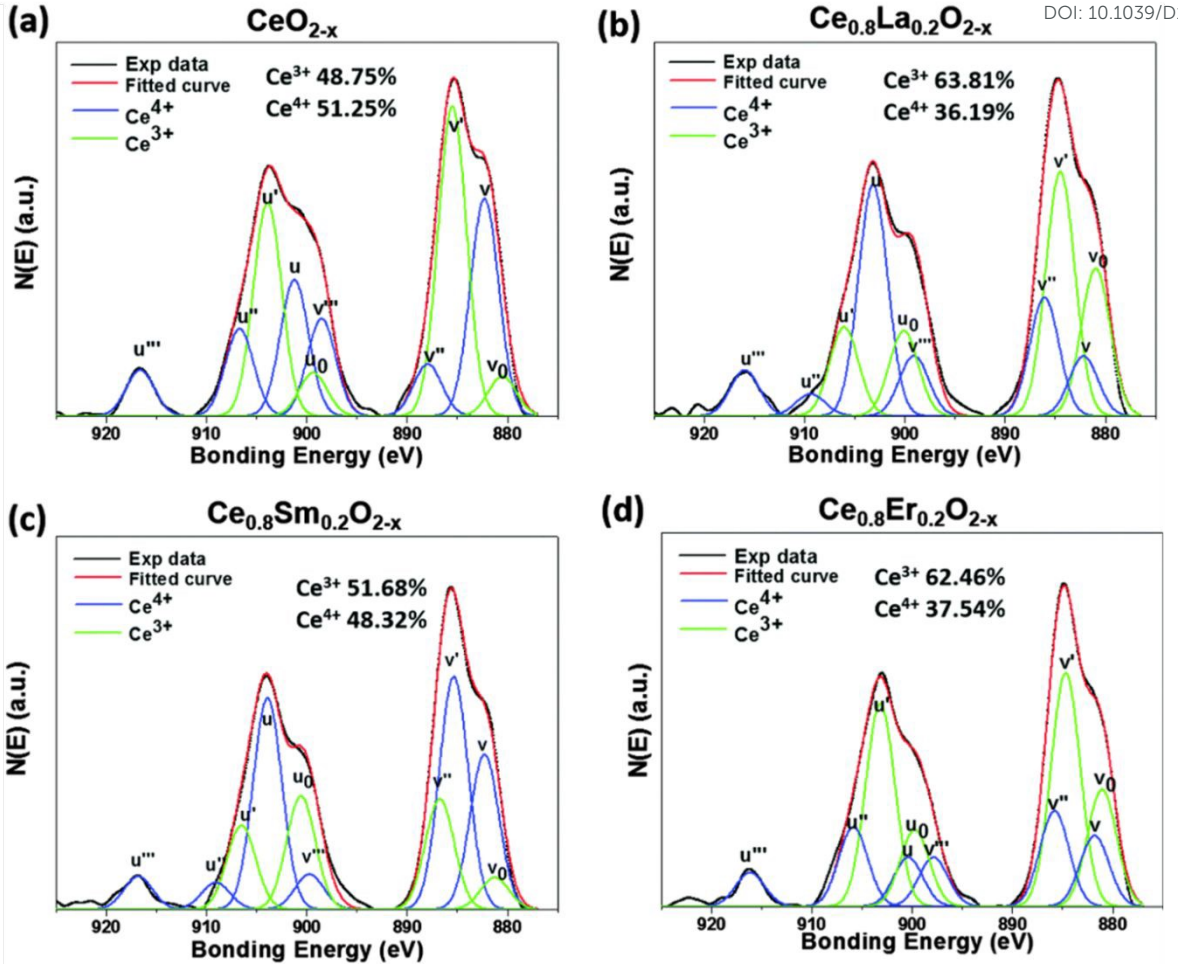

Fig. 2. XPS spectrum of Ce (3d).[46] (a) pure dextran CNPs, (b) 20 mole% lanthanum doped CNPs, (c) 20 mole% samarium doped CNPs, and (d) 20 mole% erbium doped CNPs.

2.1.2 Hydrothermal methods

Table 2 summarises hydrothermal methods used to synthesise cerium oxide nanoparticles. The main differences between precipitation and hydrothermal methods are temperature and pressure. Trenque et al.[37] suggested the morphology of the resulting nanoceria could be manipulated by different parameters in the hydrothermal methods (Fig 2A). At the same reactant concentration of cerium (III) nitrate hexahydrate and sodium hydroxide, cerium oxide nanorods could be synthesised by 6-hours heating at 100 °C, while cerium oxide nanocubes were produced by 24-hours incubation at 180 °C in teflon-lined stainless steel autoclave. When replacing sodium hydroxide with ammonium hydroxide, truncated octahedra and polyhedral nanoceria have been observed under TEM. Besides, the morphology of cerium oxide could also change from truncated octahedra to octahedra by reducing the concentration of ammonium

View Article Online
DOI: 10.1039/D1TB01091C

hydroxide. Another study indicated that polyhedral nanoceria have a higher Ce^{3+} ratio (25.3%) on the surfaces than cerium oxide nanorods (24.3%) and cerium oxide nanocubes (23.3%) (Fig 2B)[47]. In a study by Liu and coworkers,[48] cerium oxide nanocubes at size of 5 nm were synthesised from ammonium cerium (IV) nitrate and acetic acid. Cerium oxide nanocubes (100% of Ce^{4+} on the surface) were successfully encapsulated inside the reductive apoferritin (AFt–CeO_2), which increased the percentage of Ce^{3+} on the surface of cerium oxide nanoparticles from 0% to 70%. They also investigated the ROS scavenging ability of this nanoceria. Results indicated that AFt–CeO_2 had better ROS scavenging efficiency (70%) than cerium oxide nanocubes (20%) in H_2O_2-treated HepG2 cells.

Table 2. Synthesis of cerium oxide nanoparticle using hydrothermal methods.

Precursors		Reactant		Temp.	Time (hours)	Size (nm)	Surfactant /coating	Morphology	Valence states	Ref.
Cerium (III) nitrate hexahydrate (mol/L)	0.05	Sodium hydroxide (mol/L)	6	180	24	5-60	N/A	Nanocubes	Ce3+ & Ce4+	37
	0.05		6	100	6	(7-9) × (50-200)		Nanorods		
	0.05	Ammonium hydroxide (mol/L)	6	180	24	3-20		Nanocubes & Nano truncated octahedra		
	0.17		0.68	180	24	6-35		Nano-octahedra		
	0.03	Trisodium phosphate (mol/L)	0.0025	180	10	150-260		Submicronic octahedra		
	0.13	Sodium hydroxide (mol/L)	11	90	24	30 × (25-200)	N/A	Nanorods	Ce3+ (24.3%)	47
			1.8	90	24	38		Nano Polyhedra	Ce3+ (25.3%)	
			11	180	24	12.5		Nanocubes	Ce3+ (24.3%)	
Ammonium cerium (IV) nitrate (mol/L)	0.06	Acetic acid (mol/L)	2.2	220	12	5-10	Apoferritin	Nanocubes	Ce3+ (70%)	48

View Article Online
DOI: 10.1039/D1TB01091C

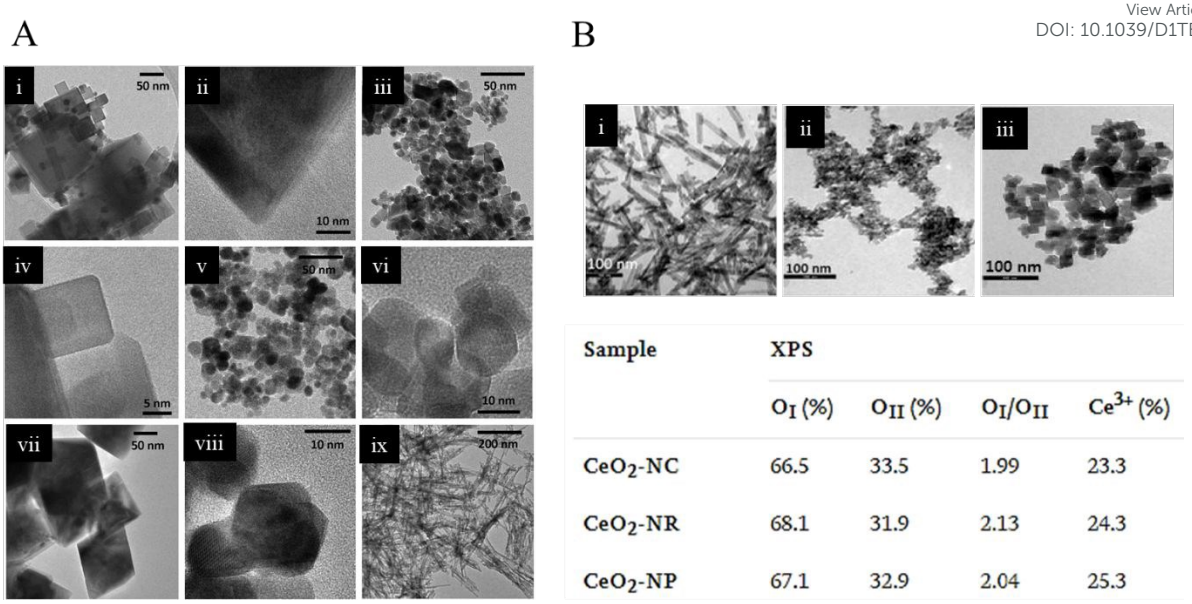

Sample	XPS			
	O_I (%)	O_{II} (%)	O_I/O_{II}	Ce^{3+} (%)
CeO_2-NC	66.5	33.5	1.99	23.3
CeO_2-NR	68.1	31.9	2.13	24.3
CeO_2-NP	67.1	32.9	2.04	25.3

Fig. 3. TEM images of cerium oxide nanoparticle synthesised by hydrothermal methods (A) TEM and HRTEM images of the various morphologies of nanoceria synthesised by Trenque et al. (i and iv) nanocubes (NCs), (vii and ii) submicronic octahedra (SOs), (v and viii) nano-octahedra (NOs), (iii and vi) mixture of nanocubes and truncated nano-octahedra (NCOs) and (ix) nanorods (NRs).[37] **(B)** TEM images and XPS data of the various morphologies of nanoceria synthesised by Lykaki et al. (i) nanorods, (ii) nano polyhedra, (iii) nanocubes [47]

2.1.3 Solvothermal methods

Table 3 summarises solvothermal methods used to synthesise cerium oxide nanoparticles. Different to the hydrothermal method, solvothermal uses organic solvents as the reaction solution to produce nanomaterials of various sizes and shape under high temperature and pressure.[49] Devaraju and coworkers presented a quick solvothermal method to prepare nanoceria. They investigated the effectivity of incubation time on the size of the nanoceria. Cerium (III) chloride heptahydrate and cerium (III) nitrate hexahydrate were used to synthesise the rodlike and spherelike cerium oxide respectively. The results indicated that thermal treatments of nanoceria at 400 °C for 20 min in batch reactor grew the diameter of rodlike cerium oxide to 500-1000 nm, from 10-20 nm with 5 min calcination. The size of spherelike cerium oxide was also increased from 100-200 nm to 500-600 nm. Besides, their results suggested that particle size could be affected by the solubility of the starting materials in different organic solvents. Rodlike nanoceria prepared in ethanol solution (200-500 nm) exhibited a smaller diameter than in methanol solution (500-800 nm) (Fig 3)[40]. In a different

View Article Online
DOI: 10.1039/D1TB01091C

study, Camacho-Ríos et al.[50] sought to synthesise the nanoceria via solvothermal method with the application of ethylenediaminetetraacetate acid (EDTA), citric acid and ascorbic acid as surface capping/stabilising agents. TEM images showed that citric acid-stabilised nanoceria has the best dispersion with particle size around 7-9 nm and quasi-spherical shape. Importantly, Ce^{4+} (27%) and Ce^{3+}(22%) was detected on the surface of cerium oxide nanoparticles.

Table 3. Synthesis of cerium oxide nanoparticle using solvothermal methods.

Precursors		Reactant		Temp.	Time (min.)	Size (nm)	Surfactant /coating	Morphology	Valence states	Ref.
Cerium (III) chloride heptahydrate (mol/L)	0.21	Ethanol	100%	400	5	(10-20) × (50-100)	N/A	Nanorods	Ce3+ & Ce4+	40
		Ethanol		400	10	(30-50) × (500-1000)		Nanorods		
		Ethanol		400	15	(200-500) × (1000-2000)		Nanorods		
		Ethanol		400	20	(200-500) × (1000-2000)		Nanorods		
		Ethanol		500	60	(200-500) × (1000-2000)		Nanorods		
		Methanol	100%	500	60	(500-800) × (1000-2000)		Nanorods		
Cerium (III) nitrate hexahydrate (mol/L)	0.25	Ethanol	100%	400	5	100-200		Nanosphere		
		Ethanol		400	10	150-300		Nanosphere		
		Ethanol		400	15	300-500		Nanosphere		
		Ethanol		400	20	500-600		Nanosphere		
		Ethanol		500	60	300-500		Nanosphere		
		Methanol	100%	500	60	400-500		Nanosphere		
Cerium (III) nitrate hexahydrate (mol/L)	0.08	Ethanol	90%	190	24	6	Citric acid	Nanosphere	Ce3+ (27%) & Ce4+ (22%)	50
				190	24	6	Ascorbic acid	Nanosphere	N/A	
				190	24	6	EDTA	Nanosphere		
				160	24	6	Citric acid	Nanosphere		
				160	24	6	Ascorbic acid	Nanosphere		
				160	24	6	EDTA	Nanosphere		

View Article Online
DOI: 10.1039/D1TB01091C

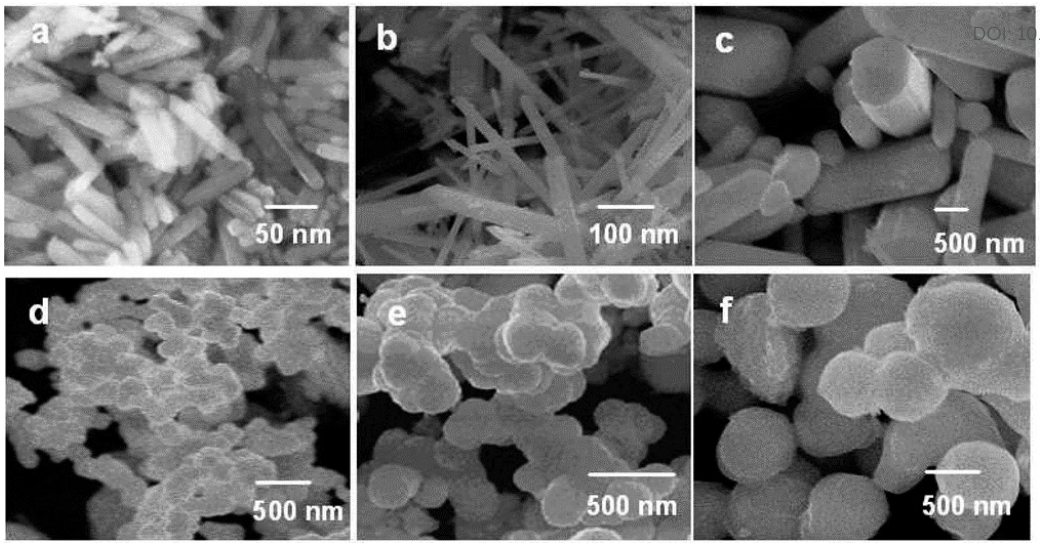

Fig 4. Field Emission Scanning Electron Microscope images of as-prepared samples using $CeCl_3 \cdot 7H_2O$ (a−c) and $Ce(NO_3)_3 \cdot 6H_2O$ and (d−f) as starting materials in ethanol at 400 °C for 5 min (a and d), 10 min (b and e), and 20 min (c and f)[40].

2.1.4 Micro emulsification micelle methods

Table 4 summarises micro emulsification micelle methods used to synthesise cerium oxide nanoparticles. Micro-emulsion is a balance system including aqueous phase, oil phase and surfactant. Zhang et al. employed the microemulsion technique to prepare nanoceria.[51] Subsequently, the resulting nanoceria were annealed at 350 °C or 600 °C for two hours. The results indicated that increasing temperature decreases the size of the particles from 65 nm to 6 nm. Besides, X-ray absorption spectra (XAS) showed the increasing Ce^{4+} on the surface of the nanoceria when the annealing at a higher temperature and changed entirely to Ce^{4+} when the annealing temperature reach to 500 °C. Additionally, Sathyamurthy and coworkers prepared well-defined polyhedral nanocerias using the reverse micellar method. The findings of this study showed that the narrow size distribution with the average size of 5 nm was achieved and physical chemical properties of nanocerias was retained by using reverse micellar method[52].

View Article Online
DOI: 10.1039/D1TB01091C

Table 4. Synthesis of cerium oxide nanoparticle using micro emulsification micelle methods.

Precursors		Reactant		Temp.	Time (hours)	Size (nm)	Surfactant/coating	Morphology	Valence states	Ref.
Cerium(III) nitrate hexahydrate (mol/L)	0.5	Ammonium hydroxide (mol/L)	2.8	350	2	65	Cetyltrimethy lammonium bromide (CTAB)	Nanosphere	Ce3+ & Ce4+	51
			2.8	600	2	6-8				
	0.4	Sodium hydroxide (mol/L)	1.7	Room tempterature	1	3-5	n-octane, CTAB, 1-butanol	Nano polyhedra	N/A	52

2.2 Green synthesis methods

Table 5 summarises diferent green methods used to synthesise cerium oxide nanoparticles. High dosage of cerium oxide nanoparticles synthesised by conventional chemical method showed cytotoxicity to many cell lines such as human bronchial epithelium cells[53], macrophages[54], human fibroblast[55] and some other cancel cells[56, 57]. Some studies showed that ceria nanorod exhibited stronger cytotoxicity than other shape of the nanoceria.[58, 59] In a study by Forest et al.[50], nanoceria at around 5 to 8 nm was synthesised by hydrothermal methods. The resulting nanoceria at the concentration of 30 µg/ml increased the production of TNF-α and caused cytotoxicity to RAW264.7. Besides, Cheng et al.[60] developed nanoceria (around 20-30 nm) by hydrothermal methods. The resulting nanoceria displayed a significant cytotoxicity on human hepatoma SMMC-7721 cells at the concentration of 50 µg/ml. Moreover, Franchi et al.[55] showed that commercial nanoceria at concentration of 10 µg/ml (25 nm, Sigma-Aldrich) caused oxidative DNA damage to human fibroblast.

To improve the biocompatibility of nanoceria at high dosage, the green synthesis of cerium oxide nanoparticles has received extensive attention.[61] These eco-friendly bio-directed methods employed nature matrices as stabilising agents to improve the biocompatibility of the nanoceria. (Table 6) Many plant extracts, nutrient and fungus products have been reported used in the green synthesis of nanoceria[62]. In a study by Nourmohammadi et al.,[63] a nanoceria mixture with spherical and cylindrical particle sizes of 34 nm was synthesised via carrageenan hydrogelation. In this method, 50 ml of cerium nitrate (0.5 g/ml) solution was gradually added in 50 ml of carrageenan solution (20 mg/ml) and stirred vigorously for 8 h at 60 °C followed by calcined for 2 h at 600 °C. Carrageenan as a green material extracted from red seaweeds. It contains vinyl sulfonic acid groups that can help capture cerium ions in the solution. The cell

View Article Online
DOI: 10.1039/D1TB01091C

viability studies showed that the carrageenan hydrogel capped cerium oxide nanoparticles have no toxicity to WEHI 164 cells at the concentration below 250 µg/ml. Another study investigated the antibacterial properties of chitosan-coated nanoceria synthesised from the extract of *Sida acuta* Brum.f. leaves[64]. Extract solution of *Sida acuta* Brum.f. leaves (20 ml) was dropwise added in 80 ml of cerium nitrate solution (43.3 mg/ml) and stirred for 3 h. The particles were then washed and dried for 3 h at 200 °C followed by coating with chitosan. The results showed that the spherical hybrid nanoceria (23-90 nm) could disrupt the structure of the bacterial membrane and caused the death of bacteria. However, the biocompatibility of hybrid chitosan-CeO_2 on mammalian cells has not been investigated in this study. Fresh egg white was also used as the capping agent in the green synthesis of spherical cerium oxide nanoparticles. 25 ml of fresh egg white was gently added in equal volume of cerium nitrate (0.5 g/ml) solution. The mixture solution was stirred for 8 h at 60 °C followed by calcined for 2 h at 600 °C. The resulting nanoparticles (25 nm) showed excellent biocompatibility in fibroblast cells with concentration up to 800 µg/ml[65].

Table 5. Synthesis of cerium oxide nanoparticle using green synthesis methods.

Precursors	**Reactant**	**Surfactant/coating**	**Size (nm)**	**Morphology**	**Valence states**	**Ref.**
Cerium nitrate hexahydrate	Carrageenan	Carrageenan	18-60	Mixture of spherical, cylindrical	N/A	63
Cerium nitrate hexahydrate	Extract of Sida acuta Brum.f. leaves	Phytoconstituents from Sida acuta Brum.f. and chitosan	23-90	Spherical	N/A	64
Cerium nitrate hexahydrate	Fresh egg white	Egg white	25	Spherical	N/A	65

View Article Online
DOI: 10.1039/D1TB01091C

Table 6. Advantage and disadvantages of conventional chemical synthesis method and green synthesis method of nanoceria

Synthesis method	Advantage	Disadvantage
Conventional chemical synthesis	● Easy to operate and scale-up ● Size and shape can be tuned ● Nanoceria with high crystallinity ● More suitable for the preparation of small size nanoceria	● Organic solvent residue ● Energy and capital intensive; ● Toxic chemicals involved in the synthesis procedure
Green synthesis	● Eco-friendly ● Consume much less energy ● Good biocompatibility	● Mechanisms not clearly understood ● Nanoceria size is variable ● Lower yield

3 Anti-ROS and anti-inflammatory properties of cerium oxide nanoparticles

The coexistence of tervalent and tetravalent cerium on the surface of nanoceria contribute to its unique regenerative anti-ROS properties and its anti-inflammation ability. Some theories of regeneration properties have been discussed in this part. Besides, in vitro and in vivo experiments also showed anti-ROS and anti-inflammatory effects of cerium oxide nanoparticles.

3.1 Regenerative anti-ROS properties

Different studies have reported the anti-ROS and anti-inflammatory properties of the cerium oxide nanoparticles.[19] Basically, the anti-ROS ability of nanoceria is related to the oxygen vacancies on its surface (Ce^{3+}/Ce^{4+} state). Tervalent cerium, as an SOD-mimetic, is able to react with superoxide radicals ($O_2^{\bullet-}$) to produce the hydrogen peroxide ($Ce^{3+} + O_2^{-\bullet} + 2H^+ \rightarrow Ce^{4+} + H_2O_2$). In a study by Korsvik and coworkers,[10] the generation of H_2O_2 were measured from the nanoceria-treated $O_2^{\bullet-}$ solution. Results showed nanoceria with a higher level of Ce^{3+} (40%) have better scavenging ability of $O_2^{\bullet-}$ than the particles with lower Ce^{3+} (22%). In another study, Heckert et al. found that reducing the Ce^{3+}/Ce^{4+} ratio of nanoceria could block their SOD-mimetic activity.[66] These studies showed that the SOD-mimetic activity is mainly related to the Ce^{3+} on the surface of nanoparticles.

In addition, like catalase (CAT), tetravalent cerium can decompose H_2O_2 to water and oxygen ($2Ce^{4+} + H_2O_2 + 2OH^- \rightarrow 2Ce^{3+} + O_2 + 2H_2O$). Pirmohamed et al.[67] reported that the concentration of H_2O_2 was rapidly decreased by the treatment of nanoceria with 23 % of Ce^{4+}

View Article Online
DOI: 10.1039/D1TB01091C

on the surface. However, no CAT mimetic activity was observed on Ce^{3+} (96%) riched nanoceria. Moreover, effective production of dissolved oxygen has been detected in H_2O_2 solution when treated with high Ce^{4+} ratio of nanoceria. However, nanoceria with higher Ce^{3+} (96%) on the surface did not show effective production of dissolved oxygen. Results suggested the CAT-mimetic activity of nanoceria is related to the percentage of Ce^{4+} on their particle surface. On the other hand, research showed the H_2O_2 scavenging might also be related to Ce^{3+} on the surface of the particles ($2Ce^{3+} + H_2O_2 + 2H^+ \rightarrow 2Ce^{4+} + 2H_2O$). After incubated with H_2O_2 solution, the results indicated that an increasing number of Ce^{4+} was present on nanoceria's surface. In this case, Ce^{3+} level was reduced by the oxidation of H_2O_2, result in the rise of Ce^{4+} level and deoxidation of H_2O_2 to H_2O[66].

Although the regeneration mechanism of cerium oxide has not been fully revealed, the regenerable ROS removal mechanism of cerium oxide can still be explained by its characteristics of SOD-mimetic and the catalase-mimetic. Firstly, $O_2^{\bullet-}$ or H_2O_2 has been scavenged by Ce^{3+} with the production of Ce^{4+} and H_2O_2 or H_2O. Subsequently, H_2O_2 reacts with Ce^{4+} to form O_2 and Ce^{3+}. This cycle achieves the regeneration and ROS scavenging ability of nanoceria.

3.2 Pre-clinical anti-ROS and anti-inflammatory properties

Current studies also showed the anti-ROS ability of nanoceria in cells and animals. In a study by Xia et al.[54], the team sought to investigate the anti-ROS ability of nanoceria in diesel exhaust particles (DEP) treated macrophage. Nanoceia around 50 nm was synthesised by hydrothermal method.The ROS level in the macrophages was reduced 40% by the treatment of 25 μg/ml of nanoceria. In another study, Hirst et al.[19] indicated that 1.4 μg/ml of cerium oxide nanoparticles (5 nm) synthesised by precipitation method could scavenge almost 100% of ROS in LPS-stimulated macrophage cells. Meanwhile, nanoceria didn't induce the damage of macrophage up to 1.4 μg/ml of cerium oxide. *In vivo* studies showed administration of 500 μg/kg of cerium oxide nanoparticles reduced malonaldehyde (MDA) level in CCl_4-induced CD1 mice. Moreover, the administration of 500 μg/kg of cerium oxide nanoparticles reduced malonaldehyde (MDA) level in CCl_4-induced CD1 mice. In this study, nanoceria showed promising anti-ROS and anti-inflammation ability in LPS-stimulated macrophages without causing any damage to cells and major organs of mice. However, the relationship between Ce^{3+}/Ce^{4+} of ceria and its anti-ROS and anti-inflammatory properties haven't been investigated in this study.

View Article Online
DOI: 10.1039/D1TB01091C

Additionally, Gupta et al.[46] investigated the anti-ROS ability of nanoceria (synthesised via precipitation method) in H_2O_2 treated human umbilical vein endothelial cell (HUVEC). Results indicated that higher Ce^{3+}-containing (63%) nanoceria (0.17 μg/ml) exhibited around 2-fold higher efficiency of the ROS scavenging in HUVEC than the nanoceria (0.17 μg/ml) with lower percentage of Ce^{3+} on the surface (49%) (Fig 5A). Nanoceria (8.5 μg/ml) showed no toxicity on HUVECs and changing of surface valence state did not affect its biocompatibility Similarly, in a study by Liu et al[48], cerium oxide nanocubes was synthesised by hydrothermal method and then coated with apoferritin (Aft-CeO_2). X-ray photoelectron spectroscopy showed that Aft-CeO_2 had 70% of Ce^{3+} on the surface of the nanoceria, while the non-coated nanoceria had no Ce^{3+} on its surface. The anti-ROS study suggested Aft-CeO_2 (4.25 μg/ml) have more than three-time higher ROS scavenging efficiency than the non-coated nanoceria (4.25 μg/ml). These two studies suggest that nanoceria with high Ce^{3+}/Ce^{4+} could have enhanced anti-ROS ability.

In 2018, Chen et al.[68] synthesised nanoceria at size of 285 nm via green synthesis method. *camellia sinens* filtrate was mix with ceric ammonium nitrate at 50 °C followed by calcinating at 600 °C for 1 h to form the spherical nanoceria. These nanoceria was able to reduce the relative ROS level (25%) at the concentration of 100 μg/ml. ROS is a critical factor in many inflammatory responses.[69] Hence, nanoceria in the regulation of ROS in the body may also affect the signalling-pathway of some inflammatory cytokines. Chen at al. also investigated the anti-inflammation property of nanoceria in LPS-stimulated macrophages. Results indicated nanoceria reduce the expression of COX-2, iNOX at the concentration of 5 μg/ml. Consistently, i*n vivo* studies showed that rat serum cytokines such as TNF-α, IL-1α, IL-1β were decreased in nanoceria-treated rats. Besides, Selvaraj et al.[70] indicated that 8.6 μg/ml of nanoceria (purchased from the NanoScale corporation) reduced the overexpression of TNF-α, COX-2, iNOX, IL-1β and COX-2 in LPS-stimulated RAW264.7. Interestingly, nanoceria at this concentration increased the viability of the LPS-treated macrophages from 60% to 80%. This may be due to the lower ROS and lower inflammatory protein level, which caused less damage to the cells. Apart from that, results from MTT-based viability assay showed no significant effect on the survivability of macrophage with the concentration of ceria less than 17.2 μg/ml.

In the studies of Oró et al.[71] they also suggested that TNF-α, IL-1β, COX-2 and iNOS expression level in CCl_4-induced rat can be reduced by nanoceria (0.1 mg/kg) synthesised by precipitation method (Fig 4). These results suggested that nanoceria from different synthesis methods have a great potential to be a therapeutic agent for ROS-related and inflammatory

View Article Online
DOI: 10.1039/D1TB01091C

diseases. (Fig 5B) In addition, the progression of hepatic steatosis and liver fibrosis was inhibited by nanoceria. (Fig 5C). Nanoceria was found accumulated in the rat's spleen, liver, lungs, and kidneys after 90 minutes of the IV injection. Moreover, it was interesting that nanoceria could exist in these organs for more than eight weeks.

The studies mentioned above showed that nanoceria from different synthesis methods possesses promising anti-ROS and anti-inflammatory ability in both *in vitro* and *in vivo* studies. It also showed good biocompatibility in cells and animal organs. Overall, it is suggested that nanoceria has a great potential to be a therapeutic agent for ROS-related and inflammatory diseases.

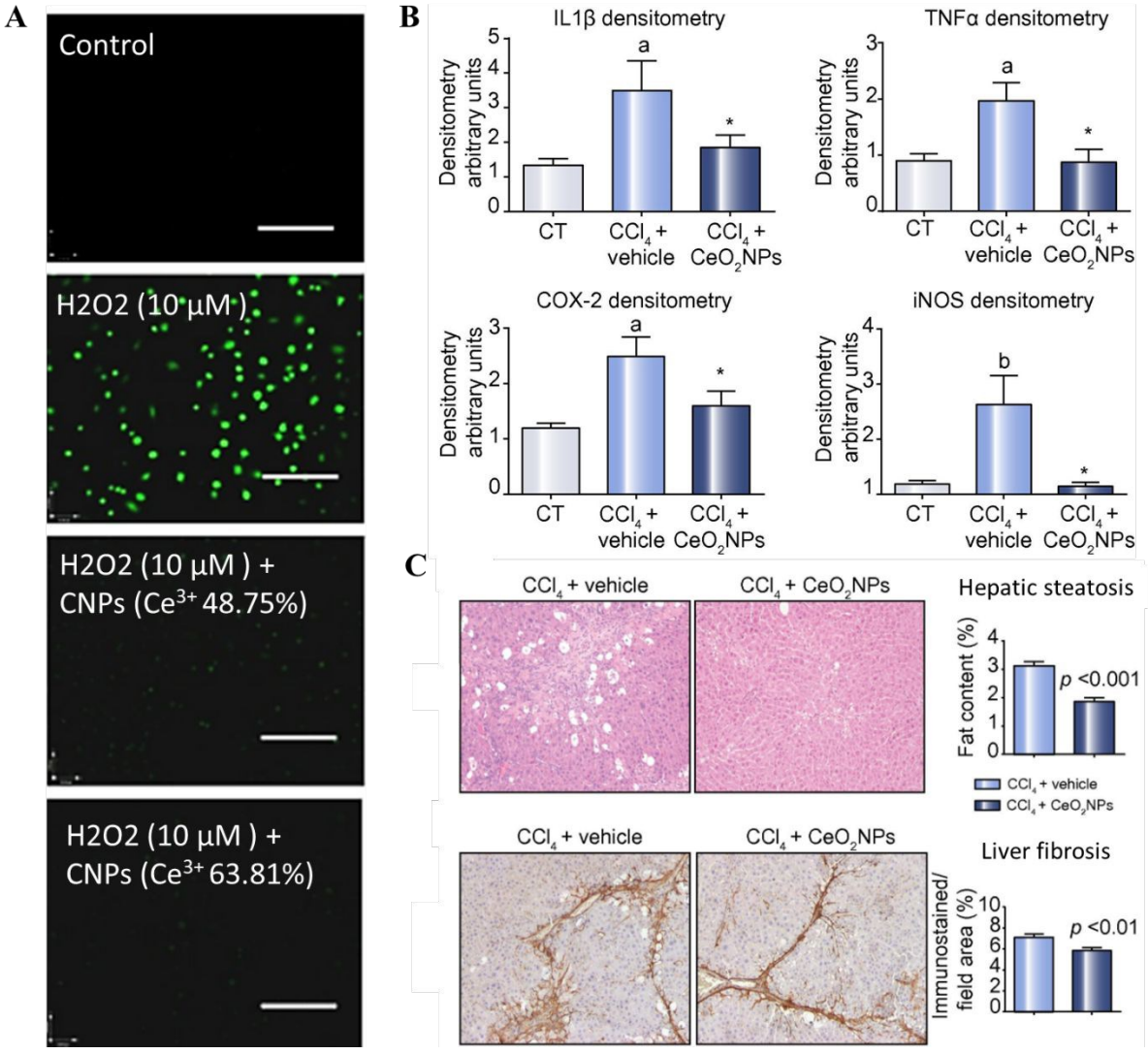

Fig 5. Anti-ROS and anti-inflammatory capabilities of nanoceria. (A) Intracellular ROS scavenging properties of CNPs evaluated by confocal microscopy. HUVEC cells treated with

View Article Online
DOI: 10.1039/D1TB01091C

1 μM of CNPs with (Ce^{3+} 40%) or without (Ce^{3+} 64%) doping exhibited decreased intracellular ROS. 10 μM of H_2O_2 was used to stimulate the ROS level. Scale bar 100 μm[46]. **(B)** Effect of CeO_2NPs on hepatic inflammation in CCl_4-treated rats. Barcharts show the densitometric analysis of all the inflammatory protein level normalised to GAPDH. Results are given as means ± SE; a, p <0.05; b, p <0.01 *vs*. control; ∗p <0.05 *vs*. CCl_4 + vehicle[71]. **(C)** Hepatic steatosis and liver fibrosis of representative liver sections obtained from CCl_4-treated rats receiving vehicle or CeO_2 NPs. The quantitative measurement showed at the right of the figure[71].

4 Conclusions and perspectives

The anti-ROS activity and their self-regeneration ability of cerium oxide nanoparticles make them excellent candidates for ROS scavengers. Besides, they are considered as alternative therapeutic agents for various chronic disease.[72-74] Nanoceria synthesised by precipitation, hydrothermal and solvothermal method has controlled size and morphology. Green synthesis method provides nanoceria a better biocompatibility. Importantly, studies indicated that more Ce^{3+} on the surface of nanoceria helps it work as an SOD-mimetic, while Ce^{4+} is responsible for the CAT-mimetic activity of the nanoceria. Moreover, results suggested that higher Ce^{3+} on the surface of nanoceria could result in a better ROS scavenging efficiency of the cerium oxide nanoparticles.

The concentration of reactants and temperature of reaction affect the physical and chemical properties of cerium oxide nanoparticles. Hence, the optimisation of their synthesis methods according to the requirements of biological applications is essential. Especially, surface percentage of Ce^{3+} and Ce^{4+} should be evaluated and reported in the future research. Heretofore, there is no detailed study on the relationship between Ce^{3+} / Ce^{4+} ratio and anti-ROS and anti-inflammatory *in vitro* and *in vivo*. Current studies have been very inconsistent in recording the Ce^{3+}/Ce^{4+} ratio, thus it is difficult to compare the anti-ROS and anti-inflammatory capability of cerium oxide from different synthesis methods. It is recommended to record the ratio by using 'percentage of Ce^{3+} or Ce^{4+}. In this way, the relationship between synthesis methods, Ce^{3+}/Ce^{4+} ratio, anti-ROS and anti-inflammatory abilities of nanoceria will be better studied and compared in the future. Besides, the toxicity of cerium oxide nanoparticles of different shapes, sizes and Ce^{3+}/Ce^{4+} ratio needs to be evaluated. The long-term effects of cerium oxide nanoparticles in the animals also need to be explored. In addition, the in vivo regeneration

ability of cerium oxide nanoparticles needs to be addressed. In the future, the targeted drug-delivery approaches[75, 76] of cerium oxide nanoparticles to inflammatory diseases needs to be further explored. Overall, the existing researches suggested that cerium oxide has the potential for various biomedical applications in the future.

Acknowledgement

This work is funded by National Health and Medical Research Council (HTT: APP1037310, APP1182347, APP2002827) and Heart Foundation (HTT: 102761).

Fig 2 and Fig 5A are reproduced from Ref. A. Gupta, S. Das, C. J. Neal and S. Seal, J Mater Chem B, 2016, 4, 3195-3202 with permission from the Royal Society of Chemistry.

Fig 3 is reproduced from Ref. I. Trenque, G. C. Magnano, M. A. Bolzinger, L. Roiban, F. Chaput, I. Pitault, S. Briançon, T. Devers, K. Masenelli-Varlot and M. Bugnet, Phys Chem Chem Phys, 2019, 21, 5455-5465 with permission from the Royal Society of Chemistry.

References

1. V. Orera, R. Merino and F. J. S. S. I. Pena, *Solid State Ion*, 1994, **72**, 224-231.
2. J. B. Hedrick and S. P. Sinha, *J Alloys Compd*, 1994, **207**, 377-382.
3. C.-H. Wang and S.-S. Lin, *Appl Catal A: Gen*, 2004, **268**, 227-233.
4. V. K. Ivanov, A. B. Shcherbakov and A. Usatenko, *Russ Chem Rev*, 2009, **78**, 855.
5. L. De Marzi, A. Monaco, J. De Lapuente, D. Ramos, M. Borras, M. Di Gioacchino, S. Santucci and A. Poma, *Int J Mol Sci*, 2013, **14**, 3065-3077.
6. Y. Ju, B. Dong, J. Yu and Y. Hou, *Nano Today*, 2019, **26**, 108-122.
7. K. Zhu, Y. Ju, J. Xu, Z. Yang, S. Gao and Y. Hou, *Acc Chem Res*, 2018, **51**, 404-413.
8. S. Das, J. M. Dowding, K. E. Klump, J. F. McGinnis, W. Self and S. J. N. Seal, *Nanomedicine*, 2013, **8**, 1483-1508.
9. I. Celardo, J. Z. Pedersen, E. Traversa and L. J. N. Ghibelli, *Nanoscale*, 2011, **3**, 1411-1420.
10. C. Korsvik, S. Patil, S. Seal and W. T. Self, *Chem Commun*, 2007, 1056-1058.
11. V. Baldim, F. Bedioui, N. Mignet, I. Margaill and J.-F. J. N. Berret, *Nanoscale*, 2018, **10**, 6971-6980.
12. J. M. Dowding, T. Dosani, A. Kumar, S. Seal and W. T. Self, *Chem Commun*, 2012, **48**, 4896-4898.
13. M. Das, S. Patil, N. Bhargava, J.-F. Kang, L. M. Riedel, S. Seal and J. J. Hickman, *Biomaterials*, 2007, **28**, 1918-1925.
14. J. Kaplan, *Nature*, 1947, **159**, 673-673.
15. D. Harrison, K. K. Griendling, U. Landmesser, B. Hornig and H. Drexler, *Am J Cardiol*, 2003, **91**, 7-11.
16. C. A. Hitchon and H. S. El-Gabalawy, *Arthritis Res Ther*, 2004, **6**, 1-14.
17. U. Z. Paracha, K. Fatima, M. Alqahtani, A. Chaudhary, A. Abuzenadah, G. Damanhouri and I. Qadri, *Virol J*, 2013, **10**, 1-9.
18. A. El-Kenawi and B. Ruffell, *Cancer cell*, 2017, **32**, 727-729.
19. S. M. Hirst, A. S. Karakoti, R. D. Tyler, N. Sriranganathan, S. Seal and C. M. Reilly, *Small*, 2009, **5**, 2848-2856.

20. M. S. Wason, J. Colon, S. Das, S. Seal, J. Turkson, J. Zhao and C. H. Baker, *Nanomedicine-Nanotechnology, Biology and Medicine*, 2013, **9**, 558-569.
21. S. M. Hirst, A. Karakoti, S. Singh, W. Self, R. Tyler, S. Seal and C. M. Reilly, *Environ Toxicol*, 2013, **28**, 107-118.
22. F. Charbgoo, M. B. Ahmad and M. J. I. j. o. n. Darroudi, *Int J Nanomedicine*, 2017, **12**, 1401.
23. Y. A. Teterin, A. Y. Teterin, A. Lebedev and I. Utkin, *J. Electron Spectros. Relat. Phenomena*, 1998, **88**, 275-279.
24. P. Trogadas, J. Parrondo and V. Ramani, *Electrochem Solid-State Lett*, 2008, **11**, B113.
25. K. Chaudhury, N. Babu, A. K. Singh, S. Das, A. Kumar and S. Seal, *Nanomedicine*, 2013, **9**, 439-448.
26. A. Clark, A. P. Zhu, K. Sun and H. R. Petty, *J Nanoparticle Res*, 2011, **13**, 5547-5555.
27. Y. Wu, R. Zhang, H. D. Tran, N. D. Kurniawan, S. S. Moonshi, A. K. Whittaker and H. T. Ta, *ACS Appl Nano Mater*, 2021, **4**, 3604–3618.
28. Y. Wu, Y. Yang, W. Zhao, Z. P. Xu, P. J. Little, A. K. Whittaker, R. Zhang and H. T. Ta, *Journal of Materials Chemistry B*, 2018, **6**, 4937-4951.
29. Y. Liu, Y. Wu, R. Zhang, J. Lam, J. C. Ng, Z. P. Xu, L. Li and H. T. Ta, *ACS Applied Bio Materials*, 2019, **2**, 5930-5940.
30. M. Nadeem, R. Khan, K. Afridi, A. Nadhman, S. Ullah, S. Faisal, Z. U. Mabood, C. Hano and B. H. Abbasi, *Int J Nanomedicine*, 2020, **15**, 5951.
31. M. Nyoka, Y. E. Choonara, P. Kumar, P. P. Kondiah and V. Pillay, *Nanomaterials*, 2020, **10**, 242.
32. E. Casals, M. Zeng, M. Parra-Robert, G. Fernández-Varo, M. Morales-Ruiz, W. Jiménez, V. Puntes and G. Casals, *Small*, 2020, **16**, 1907322.
33. B. S. Inbaraj and B.-H. Chen, *Asian J Pharm Sci*, 2020, **15**, 558-575.
34. Y.-H. Lin, L.-J. Shen, T.-H. Chou and Y.-h. Shih, *J Clust Sci*, 2020, 1-9.
35. M. Ramachandran, R. Subadevi and M. Sivakumar, *Vacuum*, 2019, **161**, 220-224.
36. F. Corsi, F. Caputo, E. Traversa and L. Ghibelli, *Front Oncol*, 2018, **8**, 309.
37. I. Trenque, G. C. Magnano, M. A. Bolzinger, L. Roiban, F. Chaput, I. Pitault, S. Briançon, T. Devers, K. Masenelli-Varlot and M. Bugnet, *Phys Chem Chem Phys*, 2019, **21**, 5455-5465.
38. M. S. Pujar, S. M. Hunagund, D. A. Barretto, V. R. Desai, S. Patil, S. K. Vootla and A. H. Sidarai, *Bull Mater Sci*, 2020, **43**, 24.
39. M. L. Hancock, R. A. Yokel, M. J. Beck, J. L. Calahan, T. W. Jarrells, E. J. Munson, G. A. Olaniyan and E. A. Grulke, *Appl Surf Sci*, 2021, **535**, 147681.
40. M. K. Devaraju, S. Yin and T. Sato, *Acs Appl Mater Inter*, 2009, **1**, 2694-2698.
41. B. Elahi, M. Mirzaee, M. Darroudi, K. Sadri and R. K. Oskuee, *Colloids Surf. B*, 2019, **181**, 830-836.
42. B. Richard, J.-L. Lemyre and A. M. Ritcey, *Langmuir*, 2017, **33**, 4748-4757.
43. Y.-H. Lin, L.-J. Shen, T.-H. Chou and Y.-h. Shih, *J Clust Sci*, 2020, DOI: 10.1007/s10876-020-01798-4.
44. P. A. Yurova, N. Y. Tabachkova, I. A. Stenina and A. B. Yaroslavtsev, *J Nanoparticle Res*, 2020, **22**, 1-15.
45. S.-X. Zhang, S.-F. Xue, J. Deng, M. Zhang, G. Shi and T. Zhou, *Biosens Bioelectron*, 2016, **85**, 457-463.
46. A. Gupta, S. Das, C. J. Neal and S. Seal, *J Mater Chem B*, 2016, **4**, 3195-3202.
47. M. Lykaki, E. Pachatouridou, S. A. Carabineiro, E. Iliopoulou, C. Andriopoulou, N. Kallithrakas-Kontos, S. Boghosian and M. Konsolakis, *Appl Catal B*, 2018, **230**, 18-28.
48. X. Liu, W. Wei, Q. Yuan, X. Zhang, N. Li, Y. Du, G. Ma, C. Yan and D. Ma, *Chem Commun*, 2012, **48**, 3155-3157.
49. R. I. Walton, *Chem Soc Rev*, 2002, **31**, 230-238.
50. M. Camacho-Ríos, J. Cristóbal-García, D. Lardizabal-Gutiérrez, I. Estrada-Guel, G. Herrera-Pérez, M. Piñón-Espitia and R. Martínez-Sánchez, *Ceram Int*, 2020.

51. J. Zhang, X. Ju, Z. Wu, T. Liu, T. Hu, Y. Xie and Z. J. C. o. m. Zhang, *Chem Mater*, 2001, **13**, 4192-4197.
52. S. Sathyamurthy, K. J. Leonard, R. T. Dabestani and M. P. Paranthaman, *Nanotechnology*, 2005, **16**, 1960-1964.
53. E.-J. Park, J. Choi, Y.-K. Park and K. J. T. Park, *Toxicology*, 2008, **245**, 90-100.
54. T. Xia, M. Kovochich, M. Liong, L. Madler, B. Gilbert, H. Shi, J. I. Yeh, J. I. Zink and A. E. Nel, *ACS nano*, 2008, **2**, 2121-2134.
55. L. P. Franchi, B. B. Manshian, T. A. de Souza, S. J. Soenen, E. Y. Matsubara, J. M. Rosolen and C. S. Takahashi, *Toxicol In Vitro*, 2015, **29**, 1319-1331.
56. W. Lin, Y.-w. Huang, X.-D. Zhou and Y. Ma, *Int J Toxicol*, 2006, **25**, 451-457.
57. M. Pešić, A. Podolski-Renić, S. Stojković, B. Matović, D. Zmejkoski, V. Kojić, G. Bogdanović, A. Pavićević, M. Mojović and A. Savić, *Chem-Biol Interact*, 2015, **232**, 85-93.
58. V. Forest, L. Leclerc, J.-F. Hochepied, A. Trouvé, G. Sarry and J. J. T. i. V. Pourchez, *Toxicol In Vitro*, 2017, **38**, 136-141.
59. Z. Ji, X. Wang, H. Zhang, S. Lin, H. Meng, B. Sun, S. George, T. Xia, A. E. Nel and J. I. J. A. n. Zink, *ACS nano*, 2012, **6**, 5366-5380.
60. G. Cheng, W. Guo, L. Han, E. Chen, L. Kong, L. Wang, W. Ai, N. Song, H. Li and H. Chen, *Toxicol In Vitro*, 2013, **27**, 1082-1088.
61. S. Iravani, *Green Chem*, 2011, **13**, 2638-2650.
62. F. Charbgoo, M. B. Ahmad and M. Darroudi, *International journal of nanomedicine*, 2017, **12**, 1401.
63. E. Nourmohammadi, R. K. Oskuee, L. Hasanzadeh, M. Mohajeri, A. Hashemzadeh, M. Rezayi and M. Darroudi, *Ceram Int*, 2018, **44**, 19570-19575.
64. R. Senthilkumar, V. Bhuvaneshwari, R. Ranjithkumar, S. Sathiyavimal, V. Malayaman and B. Chandarshekar, *Int J Biol Macromol*, 2017, **104**, 1746-1752.
65. H. Kargar, H. Ghazavi and M. Darroudi, *Ceramics International*, 2015, **41**, 4123-4128.
66. E. G. Heckert, A. S. Karakoti, S. Seal and W. T. Self, *Biomaterials*, 2008, **29**, 2705-2709.
67. T. Pirmohamed, J. M. Dowding, S. Singh, B. Wasserman, E. Heckert, A. S. Karakoti, J. E. King, S. Seal and W. T. Self, *Chem Commun*, 2010, **46**, 2736-2738.
68. G. Chen and Y. Xu, *Mater. Sci. Eng. C*, 2018, **83**, 148-153.
69. H. Blaser, C. Dostert, T. W. Mak and D. Brenner, *Trends Cell Biol*, 2016, **26**, 249-261.
70. V. Selvaraj, N. D. Manne, R. Arvapalli, K. M. Rice, G. Nandyala, E. Fankenhanel and E. R. Blough, *Nanomedicine*, 2015, **10**, 1275-1288.
71. D. Oró, T. Yudina, G. Fernández-Varo, E. Casals, V. Reichenbach, G. Casals, B. G. de la Presa, S. Sandalinas, S. Carvajal and V. Puntes, *Journal of hepatology*, 2016, **64**, 691-698.
72. S. V. Kyosseva, L. Chen, S. Seal and J. F. McGinnis, *Exp Eye Res*, 2013, **116**, 63-74.
73. V. Selvaraj, N. D. Manne, R. Arvapalli, K. M. Rice, G. Nandyala, E. Fankenhanel and E. R. Blough, *Nanomedicine*, 2015, **10**, 1275-1288.
74. J. Niu, A. Azfer, L. M. Rogers, X. Wang and P. E. Kolattukudy, *Cardiovasc Res*, 2007, **73**, 549-559.
75. W. He, N. Kapate, C. W. Shields IV and S. Mitragotri, *Adv Drug Deliver Rev*, 2020, **165**, 15-40.
76. W. Ulbrich and A. Lamprecht, *J R Soc Interface*, 2010, **7**, S55-S66.